Table II—Carbon-13 Chemical Shifts of Aminopyrine

Assignment[a]	Multiplicity[b]	Chemical Shift[c]	Relaxation Time[d], T_1, sec
C-3	s	163.6	48.9
C-5	s	150.2	30.7
C-1'	s	135.4	32.7
C-3'	d	128.9	2.54
C-4'	d	125.7	1.28
C-4	s	123.9	41.4
C-2'	d	123.0	2.32
C-8	q	43.8	2.37
C-7	q	36.6	3.23
C-6	q	10.2	4.40

[a,b,c,d] See corresponding footnotes in Table I.

centered at δ 43.8, 36.6, and 10.2 ppm were assigned to C-8, C-7, and C-6, respectively, on the basis of chemical shift theory (7), percent intensity of the signals, and comparison with the chemical shifts of I and III. The four singlets at δ 163.6, 150.2, 135.4, and 123.9 ppm observed in the SFORD spectrum of II were assigned to C-3, C-5, C-1', and C-4, respectively, on the basis of chemical shift theory (7), relaxation time, and comparison of the assignments of the corresponding carbons of I and III.

The chemical shifts of C-4 and C-5 in II were at a lower field as compared to the chemical shift of the coresponding carbons in I. This shift was due to the dimethyl amino group present at position 4 in II, which is more electronegative and bulky than the amino group present at position 4 in I. Earlier studies indicated that the electronegative group produces a downfield shift to the attached carbon of the vinyl group and an upfield shift to the next carbon of the vinyl group. The upfield shift decreases with an increase in the bulkiness of the electronegative group (7). The three doublets centered at δ 128.9, 125.7, and 123.0 ppm were attributed to C-3', C-4', and C-2', respectively, on the basis of chemical

shift theory, relaxation time, and comparison with the chemical shift of structurally related compounds I, III, V, and VI.

REFERENCES

(1) V. I. Stenberg, N. K. Narain, and S. P. Singh, *J. Heterocycl. Chem.*, **14**, 225 (1977).

(2) V. I. Stenberg, N. K. Narain, S. P. Singh, R. H. Obenauf, and M. J. Albright, *ibid.*, **14**, 407 (1977).

(3) S. P. Singh, S. S. Parmar, and V. I. Stenberg, *ibid.*, **15**, 9 (1978).

(4) S. P. Singh, S. S. Parmar, V. I. Stenberg, and S. A. Farnum, *ibid.*, **15**, 13 (1978).

(5) S. P. Singh, S. S. Parmar, V. I. Stenberg, and T. K. Akers, *ibid.*, **15**, 53 (1978).

(6) S. P. Singh, S. S. Parmar, V. I. Stenberg, and S. A. Farnum, *Spectrosc. Lett.*, **11**, 59 (1978).

(7) G. C. Levy and G. L. Nelson, "Carbon-13 Nuclear Magnetic Resonance for Organic Chemists," Wiley–Interscience, New York, N.Y., 1972, pp. 47, 62, 63, 91, 120.

(8) J. Feeney, G. A. Newman, and P. J. S. Pauwels, *J. Chem. Soc. C*, **1970**, 1842.

(9) L. F. Johnson and W. C. Jankowski, "Carbon-13 NMR Spectra," Wiley–Interscience, New York, N.Y., 1972, p. 295.

(10) K. Mullen and P. S. Pregosin, "Fourier Transform NMR Techniques: A Practical Approach," Academic, New York, N.Y., 1976, p. 65.

Evaluation of Adsorption from Dispersion Charge Profile

A. ATILLA HINCAL * and BHOGI B. SHETH ‡x

Abstract □ The evaluation of adsorption behavior from the charge profile of an adsorbent dispersion determined as a function of the adsorbate concentration was investigated by the streaming current measurement, using methylene blue and erythrosine as adsorbates and activated charcoal, microcrystalline cellulose, and polyvinylpolypyrrolidone as adsorbents. Adsorption capacity was evaluated using streaming current *versus* solute concentration plots of dye solutions and of corresponding dye solutions equilibrated with the adsorbent. It was also determined by adsorption isotherm measurement and application of the Langmuir equation. Good agreement was obtained between the adsorption capacity values from streaming current data and adsorption isotherm measurements for microcrystalline cellulose, suggesting that adsorption here was a surface phenomenon without water-soluble extractives affecting particle charge. Similar agreement was not obtained for charcoal adsorption, and this result was attributed to the unusual adsorption behavior of charcoal. Since polyvinylpolypyrrolidone gave a dispersion with high particle charge, the streaming current method could not be used with this system. The charge profile could be useful in characterizing powders for unusual adsorption behavior and possible water-soluble extractives as well as for surface area estimation in the absence of these factors.

Keyphrases □ Adsorption—evaluated from charge profile, streaming current measurement □ Charge profile—used to evaluate adsorption of dispersion, streaming current measurement □ Powders—application of charge profile for characterizing unusual adsorption behavior

New methods for screening powders for adsorption behavior are of significant pharmaceutical interest. Reports deal with the adsorption of drugs by excipients (1–3), the use of adsorbents in the treatment of accidental poisoning (4, 5), the estimation of surface area by solute adsorption (6, 7), and the control of particle charge by polyelectrolytes (8, 9).

The initial inflection point of a charge profile may be considered to represent monolayer adsorption capacity (10). Therefore, it is potentially feasible to estimate the monolayer adsorption capacity from charge profiles. This approach was utilized in systems involving chemical adsorption in an industrial application requiring surface area control of a fine particle dispersion. However, it should also

be feasible in systems showing physical adsorption where the dispersion is clean so that there are no interferences with charge measurements either by soluble contaminants of the adsorbent or by unusual adsorption behavior.

This study was concerned with the evaluation of adsorption behavior of dispersions from charge profiles obtained by the streaming current measurement using a streaming current detector. This detector provides a relatively rapid method for determination of charge profiles.

EXPERIMENTAL

The estimation of adsorption capacity from charge profiles was evaluated for the adsorption of two model solutes, an anionic dye, erythrosine[1] (I), and a cationic dye, methylene blue[2] (II), by activated charcoal[3] (III), microcrystalline cellulose[4] (IV), and polyvinylpolypyrrolidone[5] (V). Charge profiles were determined by streaming current measurements. Adsorption capacity also was determined by adsorption isotherm measurements.

Streaming Current Titrations—Streaming current titrations were done using a streaming current detector[6]. Test samples for streaming current titrations were increasing concentration dye solutions and aqueous dispersions of adsorbents in the same concentration dye solutions.

The samples were prepared as follows. Weighed amounts of the adsorbent were placed in a 250-ml conical screw-capped flask (0.1 g for III and 1 g for IV). Increasing concentration dye solutions, 250 ml, were added to each flask. The flasks were closed with a parafilm liner and screw cap. The dispersions were shaken mechanically for at least 4 hr to reach equilibrium.

Streaming current values of dye solutions and adsorbent dispersions were measured. The procedure used for the titrations was essentially similar to that reported by Shah and Sheth (11). In a typical measurement, the instrument surfaces were cleaned adequately and the sample (solution or dispersion) contained in a tall 400-ml beaker was placed in the instrument. The values were recorded after the instrument ran for 5 min to allow the reading to stabilize. Since the streaming current value is obtained in arbitrary units, it was necessary to establish a point of reference for measurement indicating that the boot and piston surfaces were clean with no solute on them. The reference point was a streaming current value of deionized water ranging from −51 to −60.

The profile for the test samples was obtained by plotting the streaming current as a function of increasing dye concentration. The profile for the solution was referred to as the solution curve, and that for the dispersion was referred to as the dispersion curve. Profiles were determined by this procedure for test systems with III and IV. Similar profiles for systems with V could not be determined because of the presence of soluble extractive that resulted in dispersions of V with a high particle charge.

Adsorption Isotherm Measurement—Weighed amounts of the adsorbent were placed in a 250-ml conical screw-capped flask (0.1 g for III and 1 g for the other two adsorbents). Increasing concentration dye solutions, 100 ml, were added to each flask, and each flask was closed with a parafilm liner and a screw cap. Then the dispersions were shaken mechanically for a sufficient time to reach equilibrium. After equilibration, the samples were centrifuged and the supernate was analyzed at room temperature (25 ± 1°) for dye concentration spectrophotometrically[7] at 526 nm for I and at 664.5 nm for II.

RESULTS AND DISCUSSION

Adsorption Isotherms—The adsorption behavior of both solutes on III and IV and of I on V essentially followed the Type I adsorption isotherm. However, the adsorption of II on V was greatly reduced and did not follow the Type I adsorption isotherm. The results of adsorption
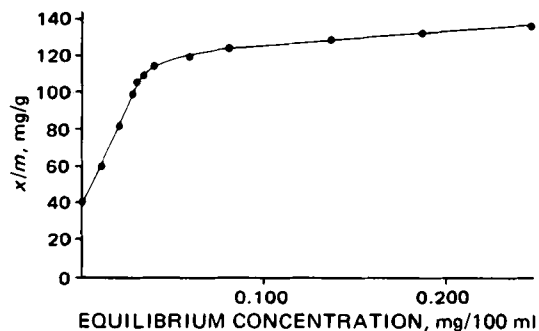
---

[1] Lot 96294, KSK Laboratories, Plainview, N.Y.
[2] Eastman Kodak Corp., Rochester, N.Y.
[3] Activated charcoal USP, American Norit Co., Jacksonville, Fla.
[4] Avicel PH-101, lot 1-90768, FMC Corp., Marcus Hook, Pa.
[5] Polyclar-AT, lot 125, GAF Corp., New York, N.Y.
[6] Hydroscan streaming current detector, Leeds & Northrup Co., North Wales, Pa.
[7] Coleman model 124 double-beam recording spectrophotometer, Perkin-Elmer, Coleman Instrument Division, Maywood, Ill.

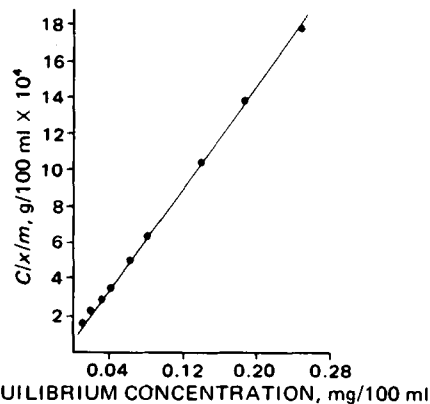**Figure 1**—*Adsorption isotherm of methylene blue on activated charcoal.*

Figure 2—*Langmuir isotherm for the adsorption of methylene blue on activated charcoal.*

studies were evaluated by the application of the Langmuir equation as follows:

$$\frac{x}{m} = \frac{k_1 k_2 C}{1 + k_1 C} \qquad (Eq. 1)$$

where C is the solute concentration at equilibrium; k_1 and k_2 are constants; x/m is the amount of solute adsorbed per gram of adsorbent; and k_2 is equivalent to $(x/m)_{max}$, the monolayer adsorption capacity.

Figure 1 shows the adsorption of II on III, and Fig. 2 shows the Langmuir plot for this system. Figures 3 and 4 show the same data for the adsorption of II by IV. Plots of $C/x/m$ versus C were linear for these systems. The Langmuir constants, k_1 and k_2, are given in Table I.

The value of k_2 may be considered as the monolayer adsorption capacity of the adsorbent for the solute. Compound III had a higher adsorption capacity for both solutes than the other two adsorbents (Table I). There was essentially no adsorption of I by IV, and II was essentially not adsorbed by V. These two adsorbents were selective adsorbents.

The adsorption of I on III was lower than that of II on the molar basis. An explanation may be found in the report of Giles and D'Silva (6), who classified the pores of finely divided III by average width into three groups on an arbitrary basis: micropores with less than 20 Å width, transitional pores between 20 and 200 Å width, and macropores that are larger than transitional pores and difficult to distinguish from the external surface.
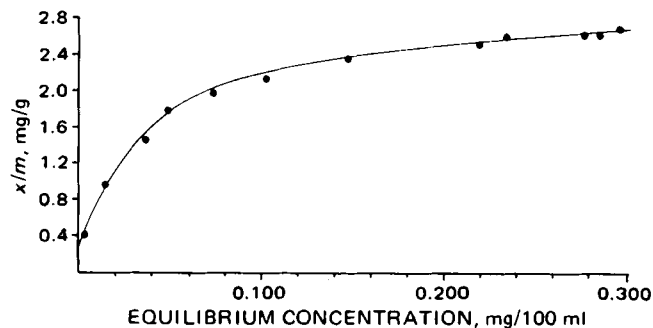

Figure 3—*Adsorption isotherm of methylene blue on microcrystalline cellulose.*

Table I—Langmuir Constants for Adsorption of Methylene Blue and Erythrosine by Activated Charcoal, Microcrystalline Cellulose, and Polyvinylpolypyrrolidone

Adsorbate	Langmuir Constant	Activated Charcoal	Microcrystalline Cellulose	Polyvinyl-polypyrrolidone
Methylene blue	k_1, 100 ml/mole	3.403×10^7	1.110×10^7	1.169×10^6
	k_2, mole/g	3.804×10^{-4}	7.924×10^{-6}	2.249×10^{-6}
Erythrosine	k_2, mole/g	1.149×10^{-4}	4.651×10^{-8}	7.987×10^{-6}
	k_1, 100 ml/mole	1.88×10^7	8.488×10^5	2.577×10^6

Table II—Comparison of Adsorption Capacity (Moles per Gram $\times 10^6$) Determined by Adsorption Isotherm Method and Streaming Current Titration for Adsorption of Methylene Blue

Adsorbent	Adsorption Isotherm	Streaming Current
Microcrystalline cellulose	7.92	7.22
Activated charcoal	380	80.2
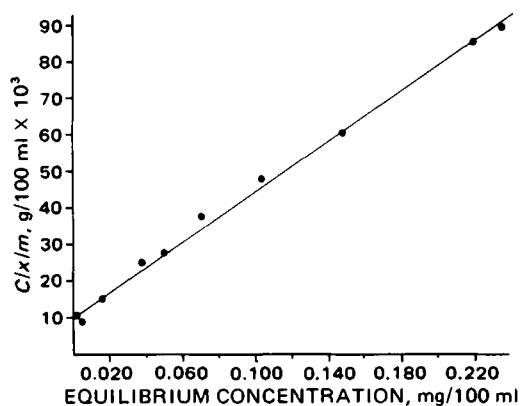
Figure 4—*Langmuir isotherm for the adsorption of methylene blue on microcrystalline cellulose.*
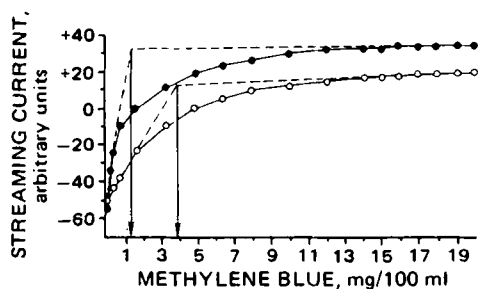
Figure 5—*Solution (●) and dispersion (O) streaming current curves for the microcrystalline cellulose-methylene blue system.*

These authors proposed that micropores were significant in the adsorption of small molecules such as nitrogen. Larger molecules would be excluded from micropores but reach some or all of the transitional pores and all of the macropores. Transitional pores were considered to have their most important influence in the adsorption of organic solutes. Therefore, the difference in adsorption behavior of I and II may be due to the difference in their molecular size, the molecule of I being much larger than II.

It was also observed that the adsorption of II caused a drop in the pH of III–II dispersions. Such behavior was noted by Bartel and Miller (12) and by Giles et al. (3). This effect was attributed to the release of hydrogen ion to the solution phase on adsorption of the dye cation.

Adsorption from Charge Profile—No literature reports were found dealing with estimation of adsorption capacity from the charge profile of a dispersion. Surface area was estimated from the charge profile in an industrial application for a system involving chemical adsorption by taking the first inflection point as the point of monolayer adsorption (13). In a chemical adsorption situation, the slope changes greatly in the streaming current charge profile at this point so that the inflection point can be determined reasonably. However, such an inflection point cannot be identified readily in a physical adsorption situation. Therefore, a

method was developed for the estimation of adsorption capacity in physical adsorption situations by utilizing the solution and dispersion curves of the system, and the adsorption capacity of II by IV and of I and II by III was evaluated.

The method is based on the determination of the inflection points of the solution and dispersion curves by regression analysis. Adsorption capacity is calculated from the difference in solute concentration at the inflection points of the two curves. Figure 5 shows the solution and dispersion curves for the IV–II system. The adsorption capacity was calculated as follows. The concentration of II at the streaming current solution curve inflection point = C_s = 1.2 mg/100 ml. The concentration of II at the streaming current dispersion curve inflection point = C_d = 3.9 mg/100 ml. Then the adsorption capacity of IV for II, milligrams of II per gram of IV, is $C_d - C_s = 3.9 - 1.2 = 2.7$ mg/g = 7.22×10^{-6} mole/g.
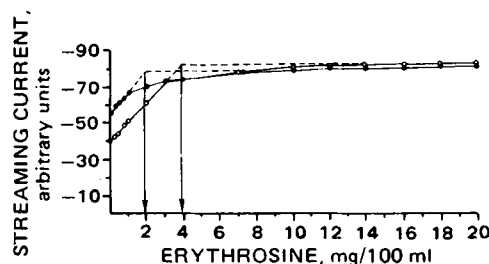
The streaming current curve for the III–II system is shown in Fig. 6. This curve is not similar to that of the IV–II system. The adsorption capacities estimated from the streaming current curves for both of these systems are given in Table II.

The type of data in Fig. 5 for the IV–II system is to be expected when there are no interferences or other complications in the streaming current measurement. The value obtained for the aqueous dispersion of IV in water without dye was −52, which was very close to the streaming current value for water. This value may be taken to indicate the absence of water-extractable material in IV. There was good agreement between the adsorption capacity values obtained by both methods (Table II). These results indicate that the developed method is applicable for physical adsorption systems where there is no interference from extractable electrolytes and the adsorption behavior is not unusual.

The estimate of adsorption capacity for the III–II system from the charge profile was also much lower than the value obtained from the adsorption isotherm. Hence, for this system, the value determined from the streaming current charge profile cannot be interpreted as representing adsorption capacity. The data for the III–II system in Fig. 6 differ from what might be expected in that the dispersion curve is higher than the
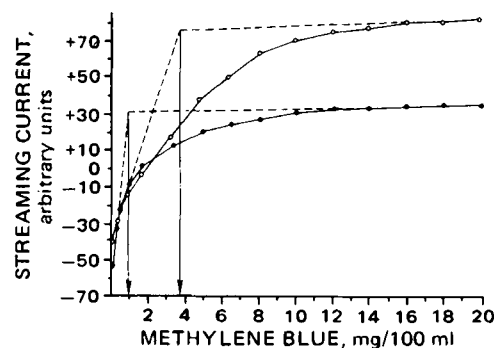
Figure 6—*Solution (●) and dispersion (O) streaming current curves for the activated charcoal-methylene blue system.*

Figure 7—*Solution (●) and dispersion (O) streaming current curves for the activated charcoal-erythrosine system.*
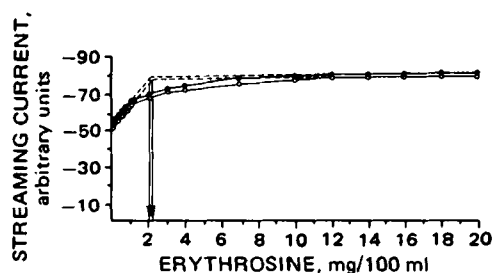
Figure 8—*Solution (●) and dispersion (○) streaming current curves for the microcrystalline cellulose–erythrosine system.*

solution curve. Typically, the dispersion curve would be below the solution curve. The reasons for this behavior are not clear, but a number of aspects of the adsorption behavior of II by III might be contributing factors. There was a drop in the aqueous dispersion pH at higher II concentrations, as discussed previously. The amount of adsorption was quite high. In measurements with the detector, the streaming current values for dispersions represent the net effect of the shearing of the double layers formed on the boot and piston surfaces as well as the double layers surrounding the dispersed particles. The contribution to the measured streaming current values from the double layers surrounding the dispersed particles may be substantially higher for dispersions with high adsorption capacity. Furthermore, higher dye concentrations were used for streaming current measurements than for adsorption isotherm measurements. At these concentrations, the dye would be expected to be in the dimer and trimer forms, with a corresponding effect on the nature of the double layer.

For the III–I system, the dispersion curve was only slightly different

from the solution curve (Fig. 7). The adsorption capacity calculated from the streaming current data was also substantially lower than that estimated from the value of k_2, the Langmuir constant for the system. Where there was no adsorption, the solution and dispersion curves were similar, as shown in Fig. 8 for the IV–I system.

REFERENCES

(1) H. Nogami, T. Nagai, and S. Wada, *Chem. Pharm. Bull.*, **18**, 342 (1970).

(2) A. L. Thakkar, W. L. Wilham, and G. Zografi, *J. Pharm. Sci.*, **59**, 1467 (1970).

(3) C. H. Giles, I. A. Easton, R. B. McKay, C. C. Patel, N. B. Shah, and D. Smith, *Trans. Faraday Soc.*, **62**, 1963 (1966).

(4) R. H. Fiser, H. M. Maetz, J. J. Treuting, and W. J. Decker, *J. Pediatr.*, **78**, 1045 (1971).

(5) A. L. Picchioni, L. Chin, and H. E. Laird, *Clin. Toxicol.*, **7**, 97 (1974).

(6) C. H. Giles and A. P. D'Silva, *Trans. Faraday Soc.*, **65**, 1943 (1969).

(7) P. T. Hang and G. W. Brindley, *Clay Clays Minerals*, **18**, 203 (1970).

(8) B. A. Matthews and C. T. Rhodes, *J. Pharm. Pharmacol.*, **20**, 204S (1968).

(9) A. N. Martin, *J. Pharm. Sci.*, **50**, 513 (1961).

(10) R. A. Nash and R. E. Haeger, *ibid.*, **55**, 829 (1966).

(11) D. G. Shah and B. B. Sheth, *Drug. Dev. Ind. Pharm.*, in press.

(12) F. E. Bartel and E. J. Miller, *J. Am. Chem. Soc.*, **44**, 1866 (1922).

(13) W. E. Gray and M. Manning, "Preprints of the Society of Photographic Scientists and Engineers Meeting," Los Angeles, Calif., 1969, p. 179.

Microencapsulation of Bitolterol for Controlled Release and Its Effect on Bronchodilator and Heart Rate Activities in Dogs

PHILLIP M. JOHN ˣ, HIROAKI MINATOYA, and FRANKLIN J. ROSENBERG

Abstract □ Spheronized cores produced by extrusion and marumerization were microencapsulated with ethylcellulose by organic phase separation to produce beads exhibiting controlled-release characteristics. *In vitro* dissolution studies indicated that the drug was released as a first-order model and that the release rates were proportional to the amount of film on the bead. The bronchodilator activity in the anesthetized dog and the heart rate effect in the unanesthetized trained dog were evaluated. Microencapsulated beads were prepared which produced controlled release as assayed by bronchodilation. The heart rate increases induced by the controlled-release formulations were gradual in onset, and the total increase in heart rate over a 6-hr period was less than that associated with the plain drug powder.

Keyphrases □ Bitolterol—microencapsulation for controlled release, effects on bronchodilator and heart rate activities, dogs □ Microencapsulation—bitolterol, controlled-release characteristics assessed, effects on bronchodilator and heart rate activities, dogs □ Dosage forms—controlled-release bitolterol formulations prepared by microencapsulation, effects on bronchodilator and heart rate activities, dogs

The properties of bitolterol, an ester of *N-tert*-butylarterenol, as a long-acting bronchodilator with reduced cardiac effects, were recently reported (1, 2). Additional

improvement in the duration of action and in the reduction of side effects was sought by preparing material exhibiting a controlled release.

Microencapsulation has been applied successfully to many areas of pharmaceutical interest. Microencapsulation as a unit operation was described and reviewed (3), as was the patent literature (4). An informative history of microencapsulation and its uses was presented (5). Most pharmaceutical work has been with irregularly shaped granules of powders or dispersed liquids, crystals, or sized granulations (6–16). This study concerns regular spherical cores in the 500–1000-μm range, encapsulated by organic phase separation.

Spherical particles were prepared (17) using an extrusion technique followed by spheronization in a marumerizer. Briefly, the drug and suitable excipients are moistened thoroughly with granulating agents and water until a damp mass is formed. The material is then passed through an extruder to produce strands of uniform diameter. The extruded material is introduced into the chamber